HAL open science

A species of magnetotactic deltaproteobacterium was detected at the highest abundance during an algal bloom

Hongmiao Pan, Yi Dong, Zhaojie Teng, Jinhua Li, Wenyan Zhang, Tian Xiao, Long-Fei Wu

To cite this version:

Hongmiao Pan, Yi Dong, Zhaojie Teng, Jinhua Li, Wenyan Zhang, et al.. A species of magnetotactic deltaproteobacterium was detected at the highest abundance during an algal bloom. FEMS Microbiology Letters, 2019, 366 (22), 10.1093/femsle/fnz253 . hal-02448980

HAL Id: hal-02448980

https://amu.hal.science/hal-02448980v1

Submitted on 22 Jan 2020

HAL is a multi-disciplinary open access archive for the deposit and dissemination of scientific research documents, whether they are published or not. The documents may come from teaching and research institutions in France or abroad, or from public or private research centers.

L'archive ouverte pluridisciplinaire **HAL**, est destinée au dépôt et à la diffusion de documents scientifiques de niveau recherche, publiés ou non, émanant des établissements d'enseignement et de recherche français ou étrangers, des laboratoires publics ou privés.

A species of magnetotactic deltaproteobacterium was detected at the highest abundance during an algal bloom

Hongmiao Pan[1,2,3,5], Yi Dong[1,2,3,5], Zhaojie Teng[1], Jinhua Li[2,4,5], Wenyan Zhang[1,2,3,5], Tian Xiao[1,2,3,5*], Long-Fei Wu[5,6]

[1] CAS Key Laboratory of Marine Ecology and Environmental Sciences, Institute of Oceanology, Chinese Academy of Sciences, Qingdao 266071, China

[2] Laboratory for Marine Ecology and Environmental Science, Qingdao National Laboratory for Marine Science and Technology, Qingdao 266237, China

[3] Center for Ocean Mega-Science, Chinese Academy of Sciences, Qingdao 266071, China

[4] Key Laboratory of Earth and Planetary Physics, Institute of Geology and Geophysics, Chinese Academy of Sciences, Beijing 100029, China.

[5] International Associated Laboratory of Evolution and Development of Magnetotactic Multicellular Organisms (LIA-MagMC), CNRS-CAS, Marseille, Beijing-Qingdao-Sanya.

[6] Aix-Marseille Univ, CNRS, LCB, Marseille, 31 chemin Joseph Aiguier, F-13402, France.

* Corresponding author:

Tian XIAO, E-mail:txiao@qdio.ac.cn; Tel.: 86-532-82898586; Fax: 86-532-82898586.

Corresponding address: Key Laboratory of Marine Ecology & Environmental Sciences, Institute of Oceanology Chinese Academy of Sciences, 7 Nanhai Rd., Qingdao 266071, CHINA.

Abstract

Magnetotactic bacteria (MTB) are a group of microorganisms that have the ability to synthesize intracellular magnetic crystals (magnetosomes). They prefer microaerobic or anaerobic aquatic sediments. Thus, there is growing interest in their ecological roles in various habitats. In this study we found co-occurrence of a large rod-shaped deltaproteobacterial magnetotactic bacterium (tentatively named LR-1) in the sediment of a

brackish lagoon with algal bloom. Electron microscopy observations showed that they were ovoid to slightly curved rods having a mean length of 6.3 ± 1.1 µm and a mean width of 4.1 ± 0.4 µm. Each cell had a single polar flagellum. They contained hundreds of bullet-shaped intracellular magnetite magnetosomes. Phylogenetic analysis revealed that they were most closely related to *Desulfamplus magnetovallimortis* strain BW-1, and belonged to the Deltaproteobacteria. Our findings indicate that LR-1 may be a new species of magnetotactic bacteria. We propose that deltaproteobacterial magnetotactic bacteria may play an important role in iron cycling and so may represent a reservoir of iron, and be an indicator species for monitoring algal blooms in such eutrophic ecosystems. These observations provide new clues to the cultivation of magnetotactic Deltaproteobacteria and the control of algal blooms, although further studies are needed.

Running title:

Occurrence of a magnetotactic deltaproteobacterium

Key words:

Magnetotactic bacteria; *Deltaproteobacteria*; Magnetosome; Eutrophic; Algal bloom; Iron

Introduction

Magnetotactic bacteria (MTB) are a heterogeneous collection of prokaryotes that can respond to magnetic fields because they produce membrane-bound magnetic intracellular magnetite (Fe_3O_4) and /or greigite (Fe_3S_4) crystals (Bazylinski and Frankel 2004). These magnetic minerals are termed magnetosomes, and are commonly arranged in chains along the long axis of the cell (Bazylinski, et al. 2013). Most MTB are ubiquitously distributed at or below the oxic–anoxic transition zone (OATZ) in freshwater and marine environments (Lin, et al. 2009, Simmons, et al. 2007, Spring, et al. 1993, Zhang, et al. 2012). Phylogenetically, all cultured and uncultured MTB have been found to be affiliated with the *Alpha-*, *Beta-*, *Delta-*, *Gamma-*, and candidate Eta-*Proteobacteria* classes within the Proteobacteria phylum (Abreu, et al. 2018, Bazylinski, et al. 2000, Ji, et al. 2017, Lefèvre, et al. 2009, Lefèvre, et al. 2011c, Lefèvre, et al. 2011e, Zhou, et al. 2012, Zhu, et al. 2010), the Nitrospirae (Journal of The Royal Society InterfaceLi, et al. 2015, Lefevre, et al. 2010, Lefèvre, et al. 2011a, Lin, et al. 2012), the Planctomycetes (Lin, et al. 2017a), the candidate Omnitrophica (Kolinko, et al. 2016) and Latescibacteria phyla (Lin and Pan 2015). It has been widely believed that MTB play important roles in the biogeochemical cycling of iron, sulfur, nitrogen and carbon (Lin, et al. 2014b, Lin, et al. 2017a).

Deltaproteobacterial MTB comprise a diverse and ecologically interactive group of sulfate-reducing bacteria (SRB). They have been found in various habitats including

freshwater rivers, moats, lakes, and wetlands (Chen, et al. 2013, Li, et al. 2019, Sakaguchi, et al. 1993, Wang, et al. 2013, Zhang, et al. 2017); in brackish lagoons and springs (Lefèvre, et al. 2011c, Lins and Farina 1999); marine intertidal zones, lagoons, and coral reefs (Chen, et al. 2015b, Teng, et al. 2018b, Zhou, et al. 2012); and in extreme hypersaline and highly alkaline environments (Lefèvre, et al. 2011b, Martins, et al. 2010). They include various morphological forms including unicells (Lefèvre, et al. 2011c), chains of 2–5 cocci (barbells) (Simmons, et al. 2006), and multicellular forms (multicellular magnetotactic prokaryotes: MMPs) (Delong, et al. 1993, Zhou, et al. 2013). Most unicellular deltaproteobacterial MTB are large rods or helical in form. Deltaproteobacterial MTB can synthesize magnetite or greigite magnetosomes, and are the only MTB able to crystallize both types within the same cell (Bazylinski, et al. 1995, Bazylizinki, et al. 1993, Chen, et al. 2015b, Kasama, et al. 2006, Kolinko, et al. 2014, Lefèvre, et al. 2011c, Spring and Bazylinski 2006, Wang, et al. 2013, Zhang, et al. 2014). Synthesis of the two types of magnetosome is controlled by two different magnetosome gene clusters and culture conditions (such as redox potential and the concentrations of sulfide and iron), as shown in pure cultures of strain BW-1, which is a deltaproteobacterium isolated from a brackish spring (Descamps, et al. 2017, Lefèvre, et al. 2011c). Most bullet-shaped magnetosomes have been found in MTB affiliated to the *Deltaproteobacteria* class and Nitrospirae phylum, which are the most deeply diverging group of the Proteobacteria and the most deeply branching phylogenetic group, respectively (Lefèvre, et al. 2011d, Lefèvre, et al. 2013a, Lin, et al. 2017b). Thus, bullet-shaped magnetosomes are considered to be the earliest to form (Lefèvre, et al. 2013a, Lin, et al. 2017b). Although *mam* genes (magnetosome genes) are conserved in all known MTB, a set of putative special genes, termed *mad* genes (**m**agnetosome **a**ssociated **d**eltaproteobacteria), appear to be highly conserved and may control magnetosome formation in deltaproteobacterial MTB (Lefèvre, et al. 2013b). Therefore, deltaproteobacterial MTB have been widely used as model organisms for investigating mechanisms of biomineralization (Lefèvre, et al. 2011c, Rahn-Lee and Komeili 2013), the evolution of magnetotaxis (Lefèvre, et al. 2013b, Nakazawa, et al. 2009), and the evolution of multicellular life (Chen, et al. 2015b).

Although coccoid alphaproteobacterial MTB predominate in most environments (Lin, et al. 2009, Pan, et al. 2008, Spring, et al. 1998), deltaproteobacterial MTB occur in some spatially heterogeneous natural environments (e.g. sediment), and there has been an increased number of reports of deltaproteobacterial MTB. However, many of these have focused on the characterization, diversity, and distribution of MMPs (Abreu, et al. 2013, Azevedo and Acosta-Avalos 2015, Chen, et al. 2016, Kolinko, et al. 2014, Leao, et al. 2017, Leao, et al. 2018, Lins and Farina 2001, Liu, et al. 2018, Simmons and Edwards 2007, Zhou, et

al. 2013). Only little literature has reported the cultivation and diversity of the unicellular deltaproteobacterial MTB (Lefèvre, et al. 2011b, Lefèvre, et al. 2011c, Li, et al. 2019, Wang, et al. 2013). Therefore, information on their characteristics and ecological roles in natural habitats is still limited.

Algal blooms occur in freshwater, marine, and brackish aquatic systems worldwide. They are promoted by eutrophication (enrichment of water with nutrients, mainly nitrogen and phosphorus) and climate change (Graneli, et al. 2008, O'Neil, et al. 2012). They are a cause of great concern because of their negative effects on biodiversity, food webs, and ultimately human health (Huisman, et al. 2018). For better understanding the influence and process of algal blooms, many studies have focused on the bacterial community composition associated with cyanobacterial aggregates (Cai, et al. 2013, Eiler and Bertilsson 2004, Tuomainen, et al. 2006), in water layer (Oliver and Ganf 2002, Wilhelm, et al. 2011, Woodhouse, et al. 2016) as well as sediment (Chen, et al. 2015a, Fan, et al. 2019, Shao, et al. 2013, Zhang, et al. 2019). Which would provide valuable information to aid in improving our ability to control cyanobacterial blooms. Although responses of some different functional microbial communities such as methanogenic microorganisms (Schwarz, et al. 2008) and algicidal bacteria (Mayali and Azam 2004) to algal blooms have been studied, the relationship between the MTB and algal bloom has never been reported.

In this study we found that a group of large rod-shaped MTB dominated in the sediment of a brackish lagoon during an algal bloom in April 2016. Microsorting combined with single cell whole genome amplification indicated that this homogenous taxonomic group represents a new species of MTB affiliated to the *Deltaproteobacteria* class.

Materials and methods

Site and MTB collection

During an algal bloom in April 2016, some surface sediments (to approximately 10 cm depth) and *in situ* water (ratio approximately 2:1) were collected from a brackish lagoon (Lvdao Lake: 37°07′N, 122°27′E) located at the top of Sanggou Bay, Shandong Province, northeastern China. Lvdao Lake is the largest lagoon (3.2 km^2) in urban Rongcheng city, and opens into the east of Sanggou Bay. Freshwater inputs to the lagoon are mainly from one large river (the Gu River) and two small rivers (the Shili and Yatou rivers). The peak of terrestrial inputs of freshwater into the lagoon occurs in summer. The nutrients entering Lvdao Lake and affecting its water quality are derived from both natural and anthropogenic sources. The sampling sites are a low tide area having a water salinity of 17‰ and a pH of 7.4. The samples were collected in 500 ml plastic bottles and were returned to the laboratory for subsequent analysis.

The MTB cells were enriched from the samples by attaching the south pole of permanent magnets outside the bottles at the water/sediment interface, as described previously (Pan, et al. 2008). The MTB were then purified using the race track method (Wolfe, et al. 1987).

Optical and electron microscopy

The number, morphology and magnetotactic behavior of the magnetic collected or purified MTB were investigated using the hanging-drop method within an artificial magnetic field. For the abundance of MTB, magnetic collected MTB samples were transferred to a 2.0 mL tube (volumes were recorded as V_1 mL). Subsequently, a 20 µL (V_2 /mL) sample of each concentrate was used to count the numbers of MTB under the microscopy (Olympus BX51) (in triplicate). The average numbers of MTB were counted as N (ind.). The abundance of MTB (A, ind./cm^3) was calculated using the formula $A = N*V_1 /V_2/Vs$, where Vs (cm^3) is the volume of sediment in each bottle. Observations were made using differential interference contrast (DIC) microscopy (Olympus BX51 equipped with a DP80 camera system; Olympus, Tokyo, Japan). Phototaxis experiments were carried out using a fluorescence microscope equipped with mercury arc UV/visible light sources (Olympus, Tokyo, Japan), as previously described (Chen, et al. 2015b).

For transmission electron microscopy (TEM) observations the purified MTB cells (not fixed or stained) were deposited on carbon-coated copper grids, rinsed with Milli-Q water, then air dried. The morphological characteristics of the MTB and the chemical composition of their magnetosomes were investigated using a HITACHI H8100 microscope operating at 115 kV, and a JEM2100 microscope operating at 200 kV and equipped for energy-dispersive X-ray spectroscopy (EDXS: Revolution), respectively (Liu, et al. 2017). The length and width of the MTB cells and magnetosomes were measured using Adobe Photoshop software. The frequency distribution of magnetosome size, calculated as (length + width)/2, and shape factor (width/length), were conducted using Origin software (Edwards 2002).

For scanning electron microscopy (SEM) the MTB cells were fixed for 1 h or overnight at 4°C in 1.25% glutaraldehyde, then transferred directly onto a 0.22 µm nucleopore polycarbonate filter (Whatman, Britain) using vacuum filtration. The samples were rinsed in 1 × PBS and dehydrated in an ethanol series (50%, 60%, 70%, 90%, and 100%: 10 min each) and soaked with isoamyl acetate for 1 h at room temperature. The cells collected on the filter were critical point dried and gold coated, and their cell surface characteristics were examined using a HITACHI S-3400N scanning electron microscope (Japan) operating at 5 kV.

Phylogenetic Analysis

For phylogenetic analysis of the MTB we combined micromanipulation with whole genome amplification (WGA) and polymerase chain reaction (PCR) amplification of the 16S rRNA gene. The use of micromanipulation in studies involving genome sequences of MTB has been reported previously (Chen, et al. 2015b, Jogler, et al. 2011, Teng, et al. 2018a, Teng, et al. 2018b). WGA of the MTB was performed using the illustra Single Cell GenomiPhi DNA Amplification Kit (GE29-1080-39; Sigma, United States) following the manufacturer's instructions, with a 2.5-h amplification (Teng, et al. 2018a, Teng, et al. 2018b). PCR amplification (Mastercycler; Eppendorf, German) was conducted using the bacterial universal primers 27f and 1492r (Lane 1991) (Sangon Biotech, Shanghai, China). The PCR products were cloned into the pMD18-T vector (TaKaRa, Dalian, China), which was transformed into competent *E. coli* TOP10 cells. Randomly chosen clones were sequenced by Nanjing Genscript Biotechnology (Nanjing, China) .

The 16S rRNA gene sequences obtained were first analyzed using the BLAST search program on the NCBI website (http://www.ncbi.nlm.nih.gov/BLAST/). The related sequences were initially aligned using the default setting of CLUSTAL W multiple alignment software, and BIOEDIT software was used to calculate the sequence identities. A phylogenetic tree was derived using the maximum-likelihood method in MEGA 6.0, with bootstrapping of 1000 replicates. The representative sequence was submitted to the GenBank database under accession number MH990263.

The sediment with rich LR-1 cells was chosen to measure total carbon (TC), total nitrogen (TN) and total organic carbon (TOC) using an elemental analyzer (Vario Macro CNS, Elementar, Germany). Major and trace element concentrations in the sediment were determined by X-ray fluorescence (XRF) spectrometry (Bruker, S8 Tiger).

Results

Occurrence of magnetotactic bacteria in Lvdao lake

At the time of sampling an algal bloom was present in Lvdao Lake, and the brackish water was green in color and contained numerous cells of *Microcystis aeruginosa* (data not shown). The sediment was dark brownish and had a sulfide odor. As expected, variously shaped MTB were observed including coccoid, vibroid, spiral, rod, and MMP forms. TEM examination showed that coccoid magnetotactic cells containing two or four elongated prismatic magnetosomes chains were often present (Fig. 1A and 1B). Magnetotactic spirilla containing single bullet-shaped magnetosome chains (Fig. 1C), rod-shaped MTB containing single tooth-shaped magnetosome chains (Fig. 1D), and oval-shaped MTB (a dividing MTB

cell) containing two prismatic magnetosomes chains (Fig. 1E) were occasionally found. Spherical mulberry-like MMPs (s-MMPs), evident because of their unique cell arrangements, were also observed using both TEM and SEM (Fig. 2). TEM investigation indicated that all MMPs cells contained bullet-shaped magnetosomes (Fig. 2A–C). SEM analysis showed that the cells in the s-MMPs were arranged in a helix (Fig. 2D and 2E). Peritrichous flagella were also found in the s-MMPs. (Fig. 2D)

Although many MTB morphologies were present in the lagoon sediment, at most sampling sites large rod-shaped magnetotactic bacteria dominated following magnetic enrichment, with a maximum abundance of approximately 10^3 ind./cm^3. DIC observations revealed that the rod-shaped magnetotactic bacterial cells have an optical "transparency dot" (white arrows in Fig. 3A), which were also observed with blue light (450–480 nm), violet light (400–410 nm), and ultraviolet light (330–385 nm) illumination under fluorescence microscope (white arrows in Fig. 3C–E). Notably neither the rod-shaped cells nor the transparency dot were observed under green light (510–550 nm) illumination (Fig. 3B). No phototaxis was evident when the rod-shaped cells were exposed to light of different wavelengths (data not shown). Both TEM and SEM observations showed that the rod-shaped cells were ovoid-to-slightly curved rods (Fig. 4A and 4C) having a mean length of 6.3 ± 1.1 µm and a mean width of 4.1 ± 0.4 µm (n = 26) (Fig. 4A). Each cell had a single polar flagellum that was almost twice the length of the cell (Fig. 4B and 4D).

Phylogenetic analysis of the dominant rod-shaped MTB

For phylogenetic analysis, approximately 100 rod-shaped MTB cells were collected using micromanipulation technology, as described in the Materials and Methods. The genomic DNA was extracted and amplified using the multiple displacement amplification (MDA) method, and the 16S rRNA gene was subsequently amplified and cloned. A total of 30 clones was picked at random for sequencing, and 29 almost complete 16S rRNA gene sequences were obtained. The sequences shared at least 97.3% sequence identity and belonged to the same OTU, indicating that the rod-shaped MTB represent a single population of likely the same species, which we designated Lvdao rod-shaped (LR-1) MTB. Phylogenetic analysis showed LR-1 is most closely related to *Desulfamplus magnetovallimortis* strain BW-1 (96.6% identity), which was isolated from a brackish spring in Death Valley National Park, California, USA (Descamps, et al. 2017, Lefèvre, et al. 2011c). They formed a clade in the *Deltaproteobacteria* class (Fig. 5). Our phylogenetic results suggest that LR-1 is a novel species of the genus *Desulfamplus*, affiliated with *Deltaproteobacteria*.

Characteristics of magnetosomes in LR-1 cells

TEM indicated that LR-1 cells are capable of producing hundreds of bullet-shaped magnetosomes (Fig. 6A1 and 6A2). The number of magnetosomes per cell ranged from 136 to 258 (average: 199; n = 10), which indicates a remarkable capacity of iron-mineralization. Although the magnetosomes formed chains along the long axis of the cell (Fig. 6A1 and 6A2), the chains appeared to bend along the curving surface of white storage globules (Fig. 6A1). A similar situation has been reported for the marine magnetotactic coccus strain MO-1 (Lefèvre, et al. 2009). Most of the magnetosomes in LR-1 cells had a bullet shape and were 65 ± 16 nm in length and 36 ± 5 nm in width (n = 100) (Fig. 6B1). Based on this, the shape factor (width/length) was approximately 0.58 ± 0.13 (Fig. 6B2). Different projected images of bullet-shaped magnetosomes having double triangle (dts) and flat top (fts) shapes were also observed in LR-1 cells (the black and white arrows in Fig. 6A2, respectively). EDXS analysis indicated that the magnetosome crystals were composed of iron and oxygen (Fig. 6C). These results indicate that LR-1 MTB can biomineralize bullet-shaped magnetite magnetosomes under natural conditions.

Physical and chemical characterization of sediment

The nutrient percentages were 720 mg/kg for TC, 460 mg/kg for TN, and 650 mg/kg for TOC. The major element concentrations of P, S and iron were 959.2 mg/kg, 625.5 mg/kg and 44,870 mg/kg, respectively. Other major and trace element concentrations in the sediment were provided in the Suplemental Information Table S1. According to reference guidelines established by the USEPA (1977) (U. S. Environmental Protection Agency 1977), the sediment with high abundance LR-1 cells in Lvdao lake was classified as nonpolluted by TN (TN<1000 mg/kg). However, TP (TP>650 mg/kg) and iron (iron>25,000) concentrations were at heavy polluted level. The results suggested that P and heavy metals are major sources of pollution in Lvdao lake.

Discussion

Two deltaproteobacterial MTB strains, *Desulfovibrio magneticus* RS-1 and *Desulfamplus magnetovallimortis* BW-1, have been isolated from sediments, the former from the Kameno River (Wakyama, Japan) and the latter from a brackish spring in Death Valley National Park (California, USA) (Descamps, et al. 2017, Sakaguchi, et al. 2002). Obligately alkaliphilic deltaproteobacterial MTB strains of *Desulfonatronum thiodismutans* (ML-1, AV-1, and ZZ-1) have been isolated and purified from three extremely alkaline hypersaline, brackish, and saline water habitats, respectively (Lefèvre, et al. 2011b). Another pure strain (SS-2), from the Salton Sea (California, USA), has also been reported (Lefèvre, et al. 2011c). Among these, only BW-1 has been shown to be capable of biomineralizing irregular greigite and/or bullet-shaped magnetite, while the others appear to synthesize only

bullet-shaped magnetite crystals under culture conditions (Lefèvre, et al. 2011b, Lefèvre, et al. 2011c, Sakaguchi, et al. 1993). Among uncultured unicellular deltaproteobacterial MTB, two groups have been found to synthesize both types of magnetosome under natural conditions in the Xi'an freshwater moat and Weiyang Lake sediments (Chen, et al. 2013, Wang, et al. 2013). Another two uncultured groups, from the freshwater Longfeng wetland of Daqing city and Weiyang Lake (named WYHR-1) only formed magnetite magnetosomes (Li, et al. 2019, Zhang, et al. 2017). In this study, although LR-1 and BW-1 share the highest 16S rRNA gene sequence identity, only one type of magnetosome (magnetite) was found in LR-1under natural condition. For BW-1, magnetite formation seems favored at low sulfide concentration (<0.3 mM) and high iron concentration (>100 μM) in the BWM medium (Descamps, et al. 2017, Lefèvre, et al. 2011c). Here, the concentrations of S in the LR-1 cells-riched sediment was 625.5 mg/kg, which corresponds to the concentration of sulfur in the BW-1 medium. Hydrogen sulfide produced by bacteria growth and sulfate reduction may not be accumulated to a very high concentration in natural shallow lake sediment because they are easily released into the overlying water and air. In addition, in the sediment sample, the iron concentration (44,870 mg/kg) was significantly higher than that in BW-1 medium. Thus, the natural environmental conditions appeared to be favorable for magnetite formation in LR-1 cells even though it may possess two sets of gene clusters like BW-1. Or LR-1 only contains one cluster genes encoding magnetite magnetosome proteins. Therefore, the genome of LR-1 and the environmental factors are needed for intensive studies.

As noted above, the average width and length of the bullet-shaped magnetosomes of the deltaproteobacterial MTB LR-1 was approximately 36 and 65 nm, respectively. This width is slightly longer than that of *Desulfamplus magnetovallimortis* BW-1 (approximately 33 nm wide (n = 61) calculated the size of magnetosomes in Fig. 2A from ref. (Descamps, et al. 2017)) and less than that of the cultured MTB deltaproteobacterial strain AV-1 (45 nm). Nevertheless, the average length of LR-1 magnetosomes is much greater and smaller than that of the BW-1 (about 47 nm in length, same measurement as above mentioned) and AV-1 (about 107 nm in length), respectively (Lefèvre, et al. 2011d). As a result, the shape factor for LR-1 (0.58) was smaller and greater than those for BW-1 (0.72) and AV-1 (0.42), respectively. In addition, it seems that only bullet-shaped magnetosomes with dts projected are for these two strains (BW-1 and AV-1) (Lefèvre, et al. 2011d), while bullet-shaped magnetosomes with both dts and fts projected co-occurred in single LR-1 cell. It's worth mentioning that LR-1 is capable of biomineralizing hundreds of bullet-shaped magnetosomes, which is more commonly observed for MTB affiliated with the Nitrospirae phylum rather than the *Deltaproteobacteria* class. These results suggest that some unknown genes differing from that in other deltaproteobacterial MTB, may be involved in determining

the size, shape, and number of bullet-shaped magnetosomes in LR-1. Also, maybe some environmental factors make the difference among of them. A more detailed investigation of this kind of MTB, as well as pure culture studies and genome information are required to elucidate it.

In this study of lagoon sediment during a cyanobacterial bloom (*Microcystis aeruginosa*) we found a homogeneous group of MTB (LR-1) that are probably sulfate reducing bacteria belonging to the *Deltaproteobacteria*. However, after the cyanobacterial bloom declined (October 2016), the abundance of LR-1 declined markedly (abundance approximately decreased from 10^3 to 4–10 ind./cm^3). This finding suggests that there may be a relationship between the proliferation of LR-1 and the occurrence of cyanobacterial blooms. One explanation for this relationship is that the cyanobacterial bloom may have led to hypoxia in Lvdao Lake. The resulting low redox potentials and high sulfide concentrations would have promoted the reproduction of SRB, which may have contributed to decomposition of the cyanobacteria (Li, et al. 2012). The sulfate-reducing LR-1 MTB would probably dominate at the sediment surface, where they may have degraded the settled cyanobacteria (Feng, et al. 2014, Wang, et al. 2014); consequently, through biogeochemical cycling they may contribute to purifying the water. A second explanation is that the water turbidity was high during the cyanobacterial bloom, restricting light availability for organisms at the sediment–water interface. Mostly, the sediment samples of MTB often stored in dim light and also the MTB be capable of escaping the damage of light with different wavelengths through the phototaxis (Azevedo, et al. 2013, Chen, et al. 2011, Chen, et al. 2015b, Li, et al. 2017, Shapiro, et al. 2011, Zhu, et al. 2010). However, as noted above, it seems that LR-1 cells did not have phototactic behavior. Thus, the high water turbidity caused by the cyanobacterial bloom may have protected the LR-1 cells from light damage, and established a favorable environment for this type of MTB. A third explanation is related to iron, which is a required trace element but also a factor limiting the growth of phytoplankton. Previous studies have shown that cyanobacteria are highly sensitive to iron deficiency, and that iron is essential to bloom formation (Fu, et al. 2019, Gress, et al. 2004, Larson, et al. 2018, Molot, et al. 2014, Paczuska and Kosakowska 2003, Parparova and Yacobi 1998, Zhou, et al. 2019). It has been suggested that ferrous iron (Fe^{2+}) diffusing from anoxic sediments is a major iron source for cyanobacteria (Molot, et al. 2014). Under aerobic conditions, iron occurs mainly as sparingly soluble Fe^{3+}. However, during a cyanobacterial bloom the overlying water and the surface sediment are anaerobic. Therefore, soluble Fe^{2+} is more stable and available in this environment. Consequently, anoxia resulting from the bloom increased the concentration of Fe^{2+}, which in turn promoted bloom formation and the proliferation of sulfate-reducing MTB. However, sulfate reduction to sulfide can also

limit ferric iron diffusion rates from anoxic sediments to the overlying water through the formation of insoluble iron sulfide (Carignan and Tessier 1988). It seems likely that LR-1 can overcome this problem in natural habitats by storing iron in their cells as magnetite rather than greigite during cyanobacterial blooms. It is also likely that the sulfide produced by sulfate reduction by LR-1 readily diffuses into the oxygenated shallow overlying water, which reduces the concentration of iron sulfide. Similar explanations have been provided in relation to the axenic deltaproteobacterial MTB strains ZZ-1, AV-1, and ML-1, isolated from extremely alkaline environments (Lefèvre, et al. 2011b). In addition, under culture conditions *Desulfamplus magnetovallimortis* strain BW-1 (the type strain most similar to LR-1) biomineralizes bullet-shaped magnetite magnetosomes at H_2S concentrations < 0.3 mM, and roughly rectangular greigite magnetosomes at H_2S concentrations > 0.3 mM (Lefèvre, et al. 2011c). This provides evidence supporting our hypothesis, although further confirmatory studies are needed.

MTB are prey for protozoa, and this is one of the likely pathways for return of iron to the environment (Bazylinski, et al. 2000, Lin, et al. 2014a, Monteil, et al. 2018). In Lvdao Lake the digestion of magnetosomes in the food vacuoles of protozoa during grazing on MTB could generate bioavailable iron for cyanobacteria. If so, deltaproteobacterial MTB may play an important role in iron cycling in such eutrophic ecosystems, and so may be a reservoir of iron and an indicator species for monitoring algal blooms.

Several cultures of unicellular axenic deltaproteobacterial MTB have been obtained (Lefèvre, et al. 2011b, Lefèvre, et al. 2011c, Sakaguchi, et al. 1993), but the isolation and culture of MMPs and most unicellular MTB remains a major challenge. This study may provide insights into how to cultivate MTB, especially magnetotacitc deltaproteobacteria. Magnetotactic bacterial-algal co-cultivation can be performed to create more favorable growth conditions for MTB such as the concentrations of O_2 and H_2S, redox gradients and light intensity. Unfortunately, it was difficult to measure some important physical and chemical characteristics of sediments and their heterogeneity *in situ*, including the oxidation reduction potential (ORP) and the concentrations of H_2S and O_2. Further research considering the relationships between MTB and algal blooms could usefully be undertaken using a sediment–water microcosmic simulation system.

Author contributions

HP, WZ, L-FW and TX designed the research. HP, YD, ZT, JL and WZ prepared samples and carried out the experiments. HP prepared the manuscript.

Founding

This study was supported by grants from the National Natural Science Foundation of China (NSFC 41776131 & 41776130) and the National Natural Science Foundation of China–Shandong Joint Fund for Marine Science Research Centers (U1706208 & U1606404).

Acknowledgements

We thank Jianhong Xu for his assistance with field sampling, and Wei Liu for assistance with SEM observations.

References

Abreu F, Leão P, Vargas G *et al.* Culture - independent characterization of a novel magnetotactic member affiliated to the Beta class of the Proteobacteria phylum from an acidic lagoon. *Environ Microbiol* 2018;**20**: 2615-24.

Abreu F, Morillo V, Nascimento FF *et al.* Deciphering unusual uncultured magnetotactic multicellular prokaryotes through genomics. *ISME J* 2013;**8**: 1055-68.

Azevedo L, Acosta-Avalos D. Photokinesis is magnetic field dependent in the multicellular magnetotactic prokaryote Candidatus Magnetoglobus multicellularis. *Antonie Van Leeuwenhoek* 2015;**108**: 579-85.

Azevedo LV, Barros HL, Keim CN *et al.* Effect of light wavelength on motility and magnetic sensibility of the magnetotactic multicellular prokaryote '*Candidatus* Magnetoglobus multicellularis'. *Antonie Van Leeuwenhoek* 2013;**104**: 405-12.

Bazylinski DA, Frankel RB. Magnetosome formation in prokaryotes. *Nat Rev Microbiol* 2004;**2**: 217-30.

Bazylinski DA, Frankel RB, Heywood BR *et al.* Controlled Biomineralization of Magnetite (Fe_3O_4) and Greigite (Fe_3S_4) in a Magnetotactic Bacterium. *Appl Environ Microbiol* 1995;**61**: 3232-9.

Bazylinski DA, Lefèvre CT, Schüler D. Magnetotactic bacteria. In: Rosenberg E., DeLong E.F., Lory S., Stackebrandt E., F. T (eds.) *The Prokaryotes*. Berlin, Heidelberg: Springer, 2013, 453-94.

Bazylinski DA, Schlezinger DR, Howes BH *et al.* Occurrence and distribution of diverse populations of magnetic protists in a chemically stratified coastal salt pond. *Chem Geol* 2000;**169**: 319-28.

Bazylizinki DA, Heywood BR, Mann S *et al.* Fe_30_4 and Fe_3S_4 in a bacterium. *Nature* 1993;**366**: 218.

Cai H-Y, Yan Z-s, Wang A-J *et al.* Analysis of the attached microbial community on mucilaginous cyanobacterial aggregates in the eutrophic Lake Taihu reveals the importance of Planctomycetes. *Microb Ecol* 2013;**66**: 73-83 (in Chinese).

Carignan R, Tessier A. The Co-Diagenesis of Sulfur and Iron in Acid Lake-Sediments of Southwestern Quebec. *Geochim Cosmochim Acta* 1988;**52**: 1179-88.

Chen C, Ma Q, Jiang W *et al.* Phototaxis in the magnetotactic bacterium *Magnetospirillum magneticum* strain AMB-1 is independent of magnetic fields. *Appl Microbiol Biotechnol* 2011;**90**: 269-75.

Chen H, Lin W, Wang Y *et al.* Diversity and magnetism of magnetotactic bacteria in lake WeiYang near Xi'an city. *Quat Sci* 2013;**1**: 88-96.

Chen N, Yang JS, Qu JH *et al.* Sediment prokaryote communities in different sites of eutrophic Lake Taihu and their interactions with environmental factors. *World J Microbiol Biotechnol* 2015a;**31**: 883-96.

Chen YR, Zhang R, Du HJ *et al.* A novel species of ellipsoidal multicellular magnetotactic prokaryotes from Lake Yuehu in China. *Environ Microbiol* 2015b;**17**: 637-47.

Chen YR, Zhang WY, Zhou K *et al.* Novel species and expanded distribution of ellipsoidal multicellular magnetotactic prokaryotes. *Environ Microbiol Rep* 2016;**8**: 218-26.

Delong EF, Frankel RB, Bazylinski DA. Multiple Evolutionary Origins of Magnetotaxis in Bacteria. *Science* 1993;**259**: 803-6.

Descamps ECT, Monteil CL, Menguy N *et al. Desulfamplus magnetovallimortis* gen. nov., sp. nov., a magnetotactic bacterium from a brackish desert spring able to biomineralize greigite and magnetite, that represents a novel lineage in the Desulfobacteraceae. *Syst Appl Microbiol* 2017;**40**: 280-9.

Edwards PM. Origin 7.0: scientific graphing and data analysis software. *J Chem Inf Comput Sci* 2002;**42**: 1270-1.

Eiler A, Bertilsson S. Composition of freshwater bacterial communities associated with cyanobacterial blooms in four Swedish lakes. *Environ Microbiol* 2004;**6**: 1228-43.

Fan Y-Y, Li B-B, Yang Z-C *et al.* Mediation of functional gene and bacterial community profiles in the sediments of eutrophic Chaohu Lake by total nitrogen and season. *Environ Pollut* 2019;**250**: 233-40.

Feng Z, Fan C, Huang W *et al.* Microorganisms and typical organic matter responsible for lacustrine “black bloom”. *Sci Total Environ* 2014;**470**: 1-8.

Fu Q-L, Fujii M, Natsuike M *et al.* Iron uptake by bloom-forming freshwater cyanobacterium Microcystis aeruginosa in natural and effluent waters. *Environ Pollut* 2019;**247**: 392-400.

Graneli E, Weberg M, Salomon PS. Harmful algal blooms of allelopathic microalgal species: the role of eutrophication. *Harmful Algae* 2008;**8**: 94-102.

Gress CD, Treble RG, Matz CJ *et al.* Biological Availability of iron to the freshwater cyanobacterium *anabaena flos-aquae*[1] . *J Phycol* 2004;**40**: 879-86.

Huisman J, Codd GA, Paerl HW *et al.* Cyanobacterial blooms. *Nat Rev Microbiol* 2018;**16**: 471-83.

Ji B, Zhang SD, Zhang WJ *et al.* The chimeric nature of the genomes of marine magnetotactic coccoid - ovoid bacteria defines a novel group of Proteobacteria. *Environ Microbiol* 2017;**19**: 1103-19.

Jogler C, Wanner G, Kolinko S *et al.* Conservation of proteobacterial magnetosome genes and structures in an uncultivated member of the deep-branching Nitrospira phylum. *Proc Natl Acad Sci U S A* 2011;**108**: 1134-9.

Journal of The Royal Society InterfaceLi J, Menguy N, Gatel C *et al.* Crystal growth of bullet-shaped magnetite in magnetotactic bacteria of the Nitrospirae phylum. *J R Soc Interface* 2015;**12**: 20141288.

Kasama T, Posfai M, Chong RKK *et al.* Magnetic properties, microstructure, composition, and morphology of greigite nanocrystals in magnetotactic bacteria from electron holography and tomography. *Am Mineral* 2006;**91**: 1216-29.

Kolinko S, Richter M, Glockner FO *et al.* Single-cell genomics reveals potential for magnetite and greigite biomineralization in an uncultivated multicellular magnetotactic prokaryote. *Environ Microbiol Rep* 2014;**6**: 524-31.

Kolinko S, Richter M, Glöckner FO *et al.* Single-cell genomics of uncultivated deep-branching magnetotactic bacteria reveals a conserved set of magnetosome genes. *Environ Microbiol* 2016;**18**: 21-37.

Lane DJ. 16S/23S rRNA Sequencing. In: Stackebrandt E, Goodfellow M (eds.) *Nucleic acid techniques in bacterial systematics*. New York: John Wiley and Sons, 1991, 115-75.

Larson CA, Mirza B, Rodrigues JLM *et al.* Iron limitation effects on nitrogen-fixing organisms with possible implications for cyanobacterial blooms. *FEMS Microbiol Ecol* 2018;**94**: fiy046.

Leao P, Chen YR, Abreu F *et al.* Ultrastructure of ellipsoidal magnetotactic multicellular prokaryotes depicts their complex assemblage and cellular polarity in the context of magnetotaxis. *Environ Microbiol* 2017;**19**: 2151-63.

Leao P, Gueiros FJ, Bazylinski DA *et al.* Association of magnetotactic multicellular prokaryotes with Pseudoalteromonas species in a natural lagoon environment. *Antonie Van Leeuwenhoek* 2018;**111**: 2213-23.

Lefevre CT, Abreu F, Schmidt ML *et al.* Moderately thermophilic magnetotactic bacteria from hot springs in Nevada. *Appl Environ Microbiol* 2010;**76**: 3740-3.

Lefèvre CT, Bernadac A, Yu - Zhang K *et al.* Isolation and characterization of a magnetotactic bacterial culture from the Mediterranean Sea. *Environ Microbiol* 2009;**11**: 1646-57.

Lefèvre CT, Frankel RB, Abreu F *et al.* Culture-independent characterization of a novel, uncultivated magnetotactic member of the Nitrospirae phylum. *Environ Microbiol* 2011a;**13**: 538-49.

Lefèvre CT, Frankel RB, Pósfai M *et al.* Isolation of obligately alkaliphilic magnetotactic bacteria from extremely alkaline environments. *Environ Microbiol* 2011b;**13**: 2342-50.

Lefèvre CT, Menguy N, Abreu F *et al.* A cultured greigite-producing magnetotactic bacterium in a novel group of sulfate-reducing bacteria. *Science* 2011c;**334**: 1720-3.

Lefèvre CT, Pósfai M, Abreu F *et al.* Morphological features of elongated-anisotropic magnetosome crystals in magnetotactic bacteria of the Nitrospirae phylum and the Deltaproteobacteria class. *Earth Planet Sci Lett* 2011d;**312**: 194-200.

Lefèvre CT, Trubitsyn D, Abreu F *et al.* Monophyletic origin of magnetotaxis and the first magnetosomes. *Environ Microbiol* 2013a;**15**: 2267–74.

Lefèvre CT, Trubitsyn D, Abreu F *et al.* Comparative genomic analysis of magnetotactic bacteria from the Deltaproteobacteria provides new insights into magnetite and greigite magnetosome genes required for magnetotaxis. *Environ Microbiol* 2013b;**15**: 2712-35.

Lefèvre CT, Viloria N, Schmidt ML *et al.* Novel magnetite-producing magnetotactic bacteria belonging to the Gammaproteobacteria. *ISME J* 2011e;**6**: 440-50.

Li H, Xing P, Wu QL. Characterization of the bacterial community composition in a hypoxic zone induced by Microcystis blooms in Lake Taihu, China. *FEMS Microbiol Ecol* 2012;**79**: 773-84.

Li J, Zhang H, Liu P *et al.* Phylogenetic and Structural Identification of a Novel Magnetotactic Deltaproteobacteria Strain, WYHR-1, from a Freshwater Lake. *Appl Environ Microbiol* 2019;**85**: 00731-19.

Li K, Wang P, Chen C *et al.* Light irradiation helps magnetotactic bacteria eliminate intracellular reactive oxygen species. *Environ Microbiol* 2017;**19**: 3638-48.

Lin W, Bazylinski DA, Xiao T *et al.* Life with compass: diversity and biogeography of magnetotactic bacteria. *Environ Microbiol* 2014a;**16**: 2646-58.

Lin W, Benzerara K, Faivre D *et al.* Intracellular biomineralization in bacteria. *Front Microbiol* 2014b;**5**: 293.

Lin W, Li J, Pan Y. Newly isolated but uncultivated magnetotactic bacterium of the phylum Nitrospirae from Beijing, China. *Appl Environ Microbiol* 2012;**78**: 668-75.

Lin W, Li J, Schüler D *et al.* Diversity analysis of magnetotactic bacteria in Lake Miyun, northern China, by restriction fragment length polymorphism. *Syst Appl Microbiol* 2009;**32**: 342–50.

Lin W, Pan Y. A putative greigite - type magnetosome gene cluster from the candidate phylum Latescibacteria. *Environ Microbiol Rep* 2015;**7**: 237-42.

Lin W, Pan Y, Bazylinski DA. Diversity and Ecology of and Biomineralization by Magnetotactic Bacteria. *Environ Microbiol Rep* 2017a;**9**: 345-56.

Lin W, Paterson GA, Zhu Q *et al.* Origin of microbial biomineralization and magnetotaxis during the Archean. *Proc Natl Acad Sci U S A* 2017b;**114**: 2171-6.

Lins U, Farina M. Organization of cells in magnetotactic multicellular aggregates. *Microbiol Res* 1999;**154**: 9-13.

Lins U, Farina M. Amorphous mineral phases in magnetotactic multicellular aggregates. *Arch Microbiol* 2001;**176**: 323-8.

Liu J, Zhang W, Du H *et al.* Seasonal changes in the vertical distribution of two types of multicellular magnetotactic prokaryotes in the sediment of Lake Yuehu, China. *Environ Microbiol Rep* 2018;**10**: 475-84.

Liu J, Zhang W, Li X *et al.* Bacterial community structure and novel species of magnetotactic bacteria in sediments from a seamount in the Mariana volcanic arc. *Sci Rep* 2017;**7**: 17964.

Martins JL, Silveira TS, Silva KT *et al.* Salinity dependence of the distribution of multicellular magnetotactic prokaryotes in a hypersaline lagoon. *Int Microbiol* 2010;**12**: 193-201.

Mayali X, Azam F. Algicidal bacteria in the sea and their impact on algal blooms 1. *J Eukaryot Microbiol* 2004;**51**: 139-44.

Molot L, Watson S, Creed I *et al.* A novel model for cyanobacteria bloom formation: the critical role of anoxia and ferrous iron. *Freshw Biol* 2014;**59**: 1323-40.

Monteil CL, Menguy N, Preveral S *et al.* Accumulation and Dissolution of Magnetite Crystals in a Magnetically Responsive Ciliate. *Appl Environ Microbiol* 2018;**84**: 02865-17.

Nakazawa H, Arakaki A, Narita-Yamada S *et al.* Whole genome sequence of *Desulfovibrio magneticus* strain RS-1 revealed common gene clusters in magnetotactic bacteria. *Genome Res* 2009;**19**: 1801-8.

O'Neil JM, Davis TW, Burford MA *et al.* The rise of harmful cyanobacteria blooms: The potential roles of eutrophication and climate change. *Harmful Algae* 2012;**14**: 313-34.

Oliver RL, Ganf GG. Freshwater Blooms. In: Whitton BA, Potts M (eds.) *The Ecology of Cyanobacteria: Their Diversity in Time and Space*. Dordrecht: Springer Netherlands, 2002, 149-94.

Paczuska L, Kosakowska A. Is iron a limiting factor of Nodularia spumigena blooms? *Oceanologia* 2003;**45**: 679–92.

Pan H, Zhu K, Song T *et al.* Characterization of a homogeneous taxonomic group of marine magnetotactic cocci within a low tide zone in the China Sea. *Environ Microbiol* 2008;**10**: 1158-64.

Parparova R, Yacobi YZ. Chelatable iron in the sub-tropical Lake Kinneret: its seasonal variation and impact on carbon uptake by natural algal assemblages and monoalgal cultures. *Aquat Sci* 1998;**60**: 157-68.

Rahn-Lee L, Komeili A. The magnetosome model: insights into the mechanisms of bacterial biomineralization. *Front Microbiol* 2013;**4**: 00352.

Sakaguchi T, Arakaki A, Matsunaga T. Desulfovibrio magneticus sp. nov., a novel sulfate-reducing bacterium that produces intracellular single-domain-sized magnetite particles. *Int J Syst Evol Microbiol* 2002;**52**: 215-21.

Sakaguchi T, Burgess JG, Matsunaga T. Magnetite formation by a sulphate-reducing bacterium. *Nature* 1993;**365**: 47-9.

Schwarz JI, Eckert W, Conrad R. Response of the methanogenic microbial community of a profundal lake sediment (Lake Kinneret, Israel) to algal deposition. *Limnol Oceanogr* 2008;**53**: 113-21.

Shao K, Gao G, Chi K *et al.* Decomposition of Microcystis blooms: Implications for the structure of the sediment bacterial community, as assessed by a mesocosm experiment in Lake Taihu, China. *J Basic Microbiol* 2013;**53**: 549-54.

Shapiro OH, Hatzenpichler R, Buckley DH *et al.* Multicellular photo - magnetotactic bacteria. *Environ Microbiol Rep* 2011;**3**: 233-8.

Simmons SL, Bazylinski DA, Edwards KJ. South-seeking magnetotactic bacteria in the Northern Hemisphere. *Science* 2006;**311**: 371-4.

Simmons SL, Bazylinski DA, Edwards KJ. Population dynamics of marine magnetotactic bacteria in a meromictic salt pond described with qPCR. *Environ Microbiol* 2007;**9**: 2162-74.

Simmons SL, Edwards KJ. Unexpected diversity in populations of the many-celled magnetotactic prokaryote. *Environ Microbiol* 2007;**9**: 206-15.

Spring S, Amann R, Ludwig W *et al.* Dominating Role of an Unusual Magnetotactic Bacterium in the Microaerobic Zone of a Freshwater Sediment. *Appl Environ Microbiol* 1993;**59**: 2397-403.

Spring S, Bazylinski DA. Magnetotactic Bacteria. In: Dworkin M., Falkow S., Rosenberg E., Schleifer KH., E.. S (eds.) *The Prokaryotes* volume 2: Ecophysiology and Biochemistry. New York, NY: Springer, 2006, 842-62.

Spring S, Lins U, Amann R *et al.* Phylogenetic affiliation and ultrastructure of uncultured magnetic bacteria with unusually large magnetosomes. *Arch Microbiol* 1998;**169**: 136-47.

Teng Z, Zhang W, Chen Y *et al.* Characterization of dominant giant rod-shaped magnetotactic bacteria from a low tide zone of the China Sea. *Chin J Oceanol Limnol* 2018a;**36**: 783-94.

Teng Z, Zhang Y, Zhang W *et al.* Diversity and Characterization of Multicellular Magnetotactic Prokaryotes From Coral Reef Habitats of the Paracel Islands, South China Sea. *Front Microbiol* 2018b;**9**: 02135.

Tuomainen J, Hietanen S, Kuparinen J *et al.* Community structure of the bacteria associated with Nodularia sp.(cyanobacteria) aggregates in the Baltic Sea. *Microb Ecol* 2006;**52**: 513-22.

U. S. Environmental Protection Agency RV, Chicago, IL. Guidelines For The Pollutional Classification Of Great Lakes Harbor Sediments. In: USEPA (ed.). Chicago, Illinois: U.S. Environmental Protection Agency, Region V, 1977.

Wang G, Li X, Fang Y *et al.* Analysis on the formation condition of the algae-induced odorous black water agglomerate. *Saudi J Biol Sci* 2014;**21**: 597-604.

Wang Y, Lin W, Li J *et al.* High diversity of magnetotactic deltaproteobacteria in a freshwater niche. *Appl Environ Microbiol* 2013;**79**: 2813-7.

Wilhelm SW, Farnsley SE, LeCleir GR *et al.* The relationships between nutrients, cyanobacterial toxins and the microbial community in Taihu (Lake Tai), China. *Harmful Algae* 2011;**10**: 207-15.

Wolfe RS, Thauer RK, Pfennig N. A 'capillary racetrack' method for isolation of magnetotactic bacteria. *FEMS Microbiol Ecol* 1987;**45**: 31-5.

Woodhouse JN, Kinsela AS, Collins RN *et al.* Microbial communities reflect temporal changes in cyanobacterial composition in a shallow ephemeral freshwater lake. *ISME J* 2016;**10**: 1337.

Zhang H, Wang F, Wang C *et al.* Detection of a Novel Magnetotactic Bacterium Belong to δ-Proteobacteria in Longfeng Wetland of Daqing City. *J Heilongjiang Bayi Agric Univ* 2017;**5**: 54-8 (in Chinese).

Zhang L, Zhao T, Wang Q *et al.* Bacterial community composition in aquatic and sediment samples with spatiotemporal dynamics in large, shallow, eutrophic Lake Chaohu, China. *J Freshwat Ecol* 2019;**34**: 575-89.

Zhang R, Chen YR, Du HJ *et al.* Characterization and phylogenetic identification of a species of spherical multicellular magnetotactic prokaryotes that produces both magnetite and greigite crystals. *Res Microbiol* 2014;**165**: 481-9.

Zhang WY, Zhou K, Pan HM *et al.* Two genera of magnetococci with bean-like morphology from intertidal sediments of the Yellow Sea, China. *Appl Environ Microbiol* 2012;**78**: 5606-11.

Zhou H, Chen X, Liu X *et al.* Effects and control of metal nutrients and species on *Microcystis aeruginosa* growth and bloom. *Water Environ Res* 2019;**91**: 21-31.

Zhou K, Zhang WY, Pan HM *et al.* Adaptation of spherical multicellular magnetotactic prokaryotes to the geochemically variable habitat of an intertidal zone. *Environ Microbiol* 2013;**15**: 1595–605.

Zhou K, Zhang WY, Yu - Zhang K *et al.* A novel genus of multicellular magnetotactic prokaryotes from the Yellow Sea. *Environ Microbiol* 2012;**14**: 405-13.

Zhu K, Pan H, Li J *et al.* Isolation and characterization of a marine magnetotactic spirillum axenic culture QH-2 from an intertidal zone of the China Sea. *Res Microbiol* 2010;**161**: 276-83.

Fig. 1 TEM images showing various morphological forms of representative MTB cells collected from Lvdao Lake. Cocci (A, B), spirilla (C), rod (D) and ovoid (E). Bars = 500 nm.

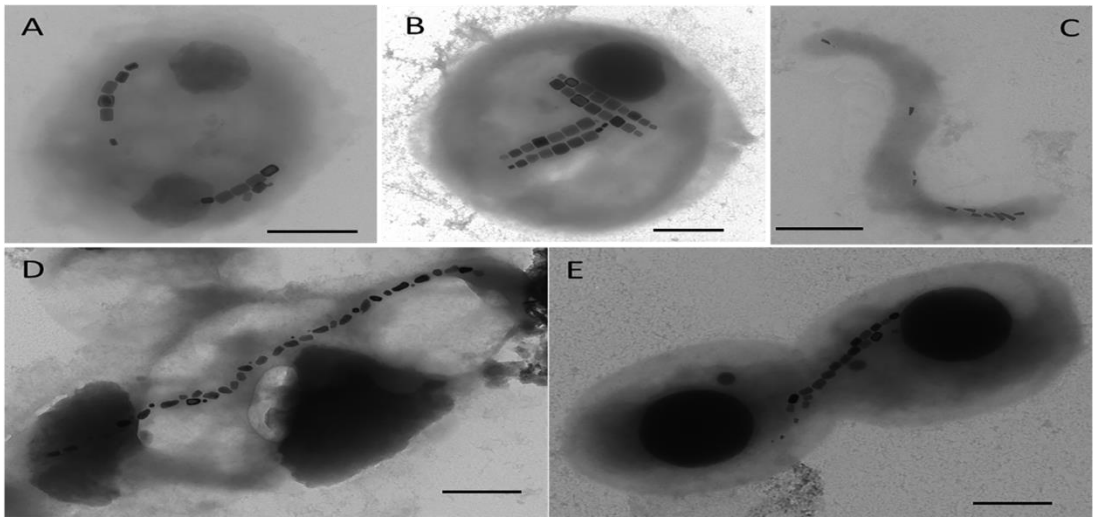

Fig. 2 TEM and SEM images of spherical mulberry-like MMPs (s-MMPs) collected from Lvdao Lake. A–C: TEM images of representative s-MMPs containing bullet-shaped magnetosomes. SEM images of s-MMPs showing flagella evident on the surface (D) and a depression in the cell surface (E). Bars = 2 µm in A, B, and C. Bars = 1 µm in D and E.

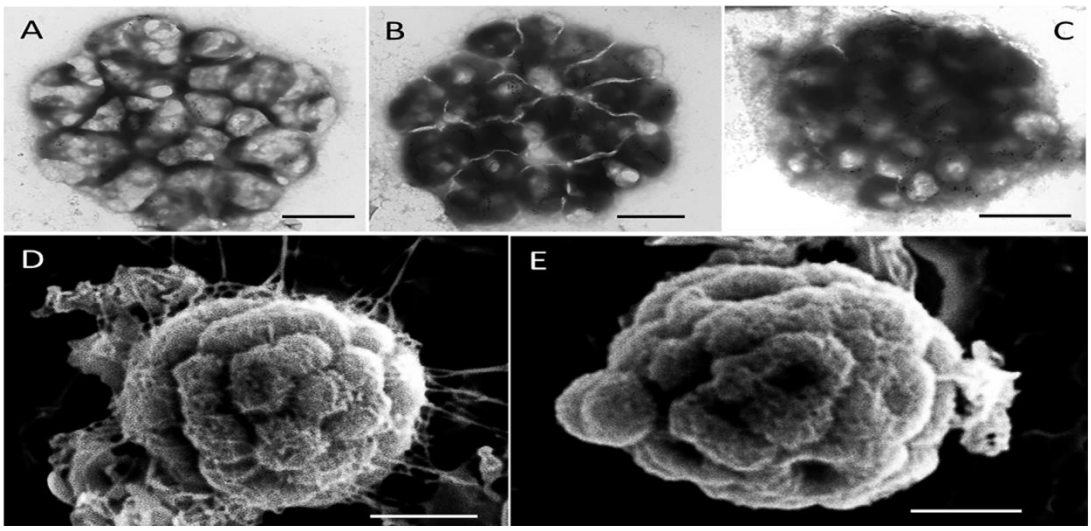

Fig. 3 The morphology and autofluorescence of rod-shaped MTB as viewed by optical microscopy. Differential interference contrast (DIC) image of rod-shaped MTB (A). In panel (A) the black arrow indicates the direction of the applied magnetic field. Panels B–E show the fluorescence of rod-shape MTB cells exposed to green light (510–550 nm) (B), blue light (450–480 nm) (C), violet light (400–410 nm) (D), and ultraviolet light (330–385 nm) (E). The white arrows indicate the optical "transparency dots". Scale bar = 10 µm for all images.

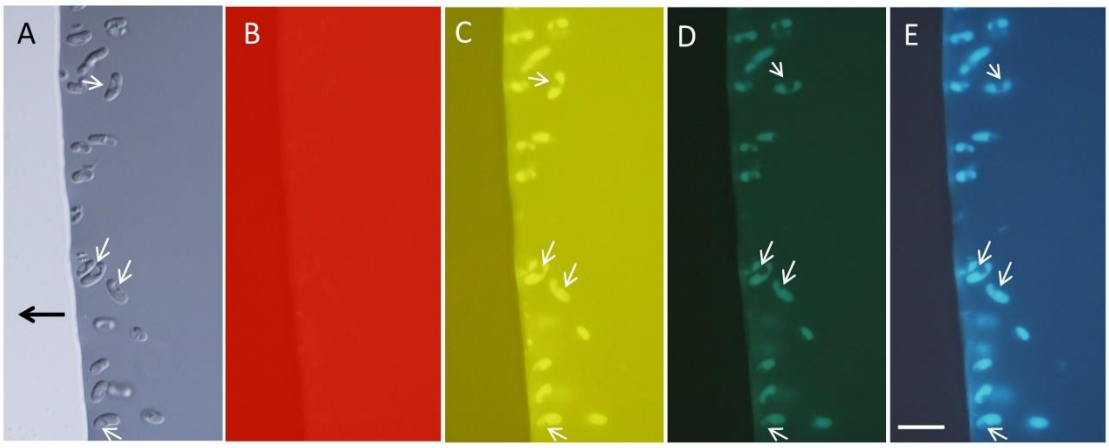

Fig. 4 Morphology of rod-shape MTB observed using TEM (A, B) and SEM (C, D), including the presence of a single flagellum (B and D). Bars = 5 µm.

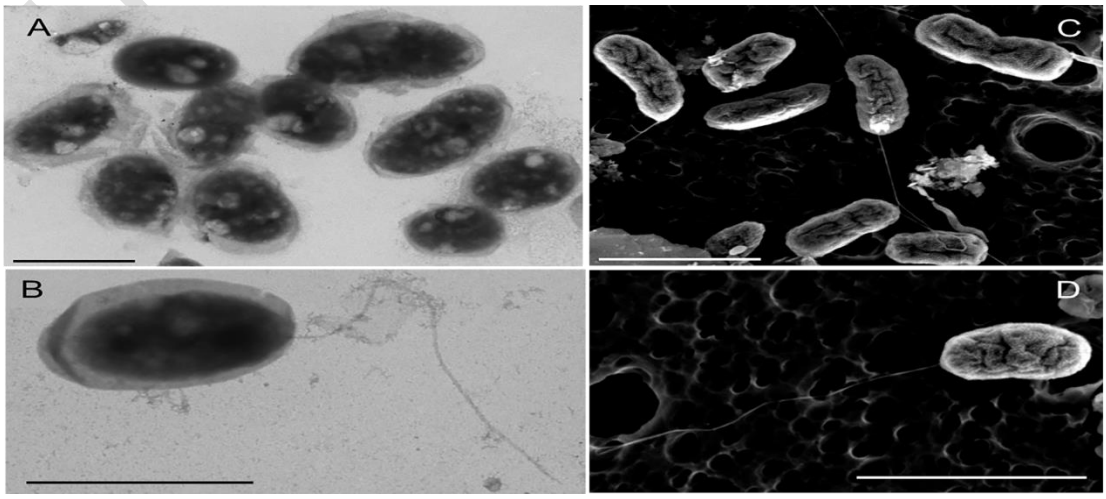

Fig. 5 Maximum-likelihood tree for LR-1 based on 16S rRNA gene sequences. The sequence determined in this study is shown in bold text. GenBank accession numbers of the sequences used are indicated in parentheses. Bootstrap values are provided. Scale bar: 0.02 substitutions per nucleotide position.

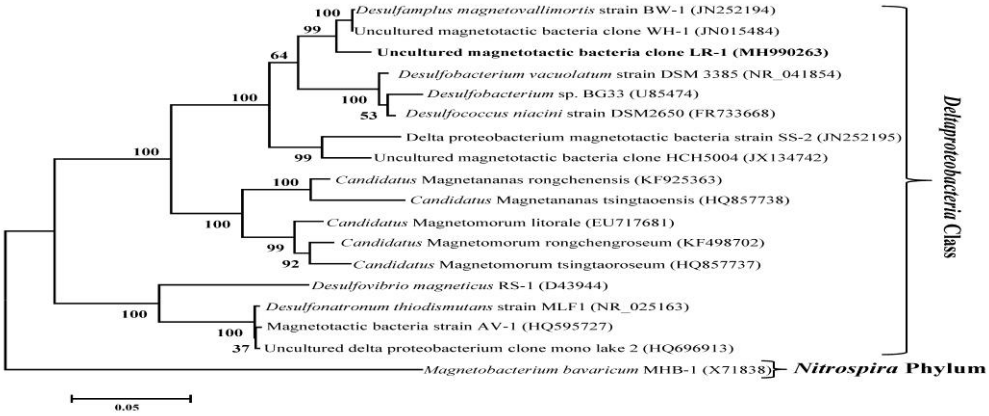
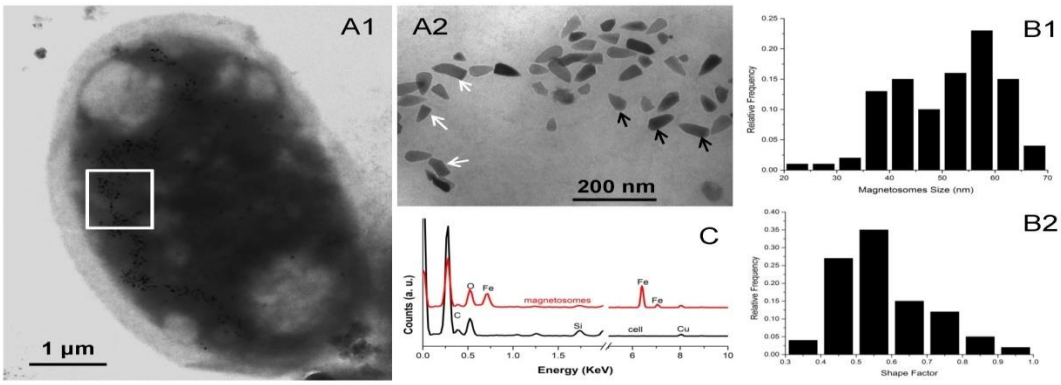
Fig. 6 Characteristics of the magnetosomes of rod-shape MTB. Rod-shape MTB cell with abundant intracellular magnetosomes (A1). A2: enlargement of the framed part of A1, showing bullet-shaped magnetosomes. Black arrows indicate the dts bullet-shaped magnetosomes and white arrows indicate the fts bullet-shaped magnetosomes. Histograms of magnetosome size (B1) and shape factor distribution (B2). Energy dispersive X-ray (EDX) analysis of magnetosomes (C). Note the peaks of iron and oxygen.